Polarforschung 70: 69 – 82, 2000 (erschienen 2002)

Evolution of Lake Nikolay, Arga Island, Western Lena River Delta, during Late Pleistocene and Holocene Time

by Georg Schwamborn[1], Andrei A. Andreev[1], Volker Rachold[1], Hans-Wolfgang Hubberten[1], Mikhail N. Grigoriev[2], Volodya Tumskoy[3], Elena Yu. Pavlova[4] and Marina V. Dorozkhina[4]

Summary: The Late Pleistocene and Holocene history of Lake Nikolay on Arga Island, western Lena River delta, is reconstructed using shallow seismic and radio-echo sounding (RES) profiles and sedimentary analyses including granulometry, biogeochemistry and pollen analysis. The main objective of this study is directed to the controversy about a glacial or a periglacial origin of Arga Island and a glacial or periglacial origin of the numerous lakes located in the western part of the Lena River delta. Determining the age and genesis of Lake Nikolay, which is the largest amongst the lakes, might mirror large parts of the history of Arga Island. Shallow seismic profiles (25 km total length) of basin fills and complementing RES profiles (23 km total length) of frozen shallow margins and a transect of sediment cores taken from one of Lake Nikolay's depo-centers to the lake margin provide evidence for lake evolution since Early Holocene time and its existence until modern times. Prior to lake evolution uppermost sediments of the second sandy terrace of the Lena River delta holding Lake Nikolay accumulated at the end of the Late Pleistocene (14,500 to 10,900 yr BP). Sediment properties suggest a fluvial environment with riverbed characteristics. After initial wet ground stages lake basin formation in the sandy environment was established at 7000 ^{14}C yr BP due to thermokarst. The onset of the thermokarst processes coincides with the regional Holocene climatic optimum according to pollen analyses. Seismic profiles reveal that under deep lake basins closed zones of unfrozen deposits (i.e. taliks) exist. This interpretation is confirmed by mathematical modeling of talik expansion. In fact, neither geological nor geophysical results are obtained, which support the hypothesis of a glacially caused morphology of the area as deduced from remote sensing techniques according to some authors. The occurrence of massive underground ice proposed by others cannot be proven until now, either.

Zusammenfassung: In der vorliegenden Arbeit wird die spät-pleistozäne und holozäne Entstehungsgeschichte des in Nord-Sibirien gelegenen Nikolay-Sees rekonstruiert. Der See befindet sich auf der Arga-Insel im westlichen Lena-Delta, einer Region die in zweifacher Hinsicht Gegenstand einer anhaltenden Kontroserve ist. Zum einen betrifft es ihre Entstehung als morphologischer Bestandteil des Lena-Deltas; es ist noch unklar, ob sie als glazial oder periglazial anzusehen ist. Zum anderen wird eine Diskussion geführt über die glaziale bzw. periglaziale Entstehungsgeschichte der zahllosen Seen, die die Arga-Insel charakterisieren. Da der Nikolay-See der größte See der Arga-Insel ist, dürfte seine Genese in großen Teilen auch die Entstehungsgeschichte der Arga-Insel und ihrer Seen widerspiegeln.

Ein datierter Seesedimentkern, biogeochemische Messungen (organischer Kohlenstoff, δ13C des organischen Kohlenstoffs) und Pollenanalysen an diesem Sedimentkern, hochauflösende seismische Stratigraphie für die Beckenfüllungen und Georadarprofile von den gefrorenen Uferbereichen stellen die Grundlage zur Rekonstruktion der Seegeschichte dar. Ergänzend stehen Lumineszenz-Alter von den sandigen Sedimenten der den See umgebenden Arga-Ablagerungen zur Verfügung.

Die Befunde ergeben eine konsistente Chronologie von der spät-pleistozänen Formation der Arga-Sande, die das heutige sedimentäre Umfeld des Sees bilden, bis zur Entstehung des Nikolay-Sees in der ersten Hälfte des Holozäns und seines Fortbestandes bis in die heutige Zeit. Die obersten sandigen Sedimente der zweiten Terrasse des Lena-Deltas in der Nähe des Nikolay-Sees entstanden demnach zum Ende des Spät-Pleistozäns (zwischen 14.500-10.900 Jahren v.H.). Nach ihren sedimentologischen Eigenschaften (Korngröße, Organik-Gehalt) werden die sandigen Sedimente als fluviale Bodenfracht eines Flusssystems gedeutet. Nach initialen Feuchtgebietsstadien setzte aufgrund von Thermokarstvorgängen um 7000 Jahre v.H. eine Seebeckeneintiefung in den sandigen Flusssedimenten ein. Der Beginn des Thermokarstes fällt nach Pollenuntersuchungen mit dem regionalen holozänen Klimaoptimum zusammen. Seismische Messungen deuten an, dass unter den tieferen Seebecken geschlossene Auftauzonen (d.h. Taliks) existieren, deren Sedimentsubsidenz nach dem Auftauen des Permafrostes alleine ausreicht, um die Beckenbildung zu erklären. Diese Interpretation wird durch ein mathematisches Modell gestützt, das die Ausbreitung des Taliks und die Beckeneintiefung gegen die Zeit simuliert.

Zusammenfassend kann festgestellt werden, daß weder die geologischen noch die geophysikalischen Ergebnisse, die hier vorgelegt werden, Thesen einer glazial entstandenen Morphologie der Arga-Insel und ihrer Seen stützen. Ebensowenig kann das Auftreten massiven Untergrundeises belegt werden, dessen Auftauen von anderen Autoren für die Einsenkung der Seebecken verantwortlich gemacht wird.

INTRODUCTION

According to GRIGORIEV (1993) the Lena River delta protuberating into the North Siberian Laptev Sea can be subdivided into three major geomorphological terraces (Fig. 1). The northeastern part of the delta (first terrace including modern floodplain levels) is assumed the „active" delta with accumulations of mainly sandy sequences and alluvial organic matter of late Holocene age (SCHWAMBORN et al. 2000a). The northwestern part consists of mainly sandy deposits (second terrace). IR-OSL datings show a Late Pleistocene age for the uppermost layers of the second terrace (KRBETSCHEK et al. this volume). Third terrace deposits are found at the southern rim of the delta plain. They consist of ice-rich peaty sand accumulations (so-called Ice Complex) overlying sequences of sandy sediments. They are of Early to Middle Pleistocene age (KRBETSCHEK et al. 2001).

Today the Lena River delta is part of the permafrost area of northern Siberia where permafrost thickness reaches 500-600 m (GAVRILOV et al. 1986). But there is a disagreement upon the extent of the ice sheet in the area during Late Pleistocene time. Especially the origin of the sandy second terrace and the age and origin of the numerous lakes located there is in discussion (ARE & REIMNITZ 2000). Viewpoints contrary interpret the history of Arga Island, which forms the main part of the second terrace, as glacial or periglacial, respectively. One view

[1] Alfred Wegener Institute for Polar and Marine Research, Research Unit Potsdam, Telegrafenberg A43, D-14471 Potsdam, Germany. <gschwamborn@awi-potsdam>, <aandreev@awi-potsdam>, <vrachold@awi-potsdam>, <hubbert@awi-potsdam>
[2] Permafrost Institute, Russian Academy of Sciences, 677018 Yakutsk, Yakutia, Russia. <grigoriev@mpi.ysn.ru>
[3] Faculty of Geology, Moscow State University, 119899 Moscow, Russia. <tumskoy@orc.ru>
[4] Arctic and Antarctic Research Institute, Bering St. 38, 199397 St. Petersburg, Russia. <lpavlova@otto.nw.ru>

Manuscript received 28 December 2000, accepted 31 July 2001

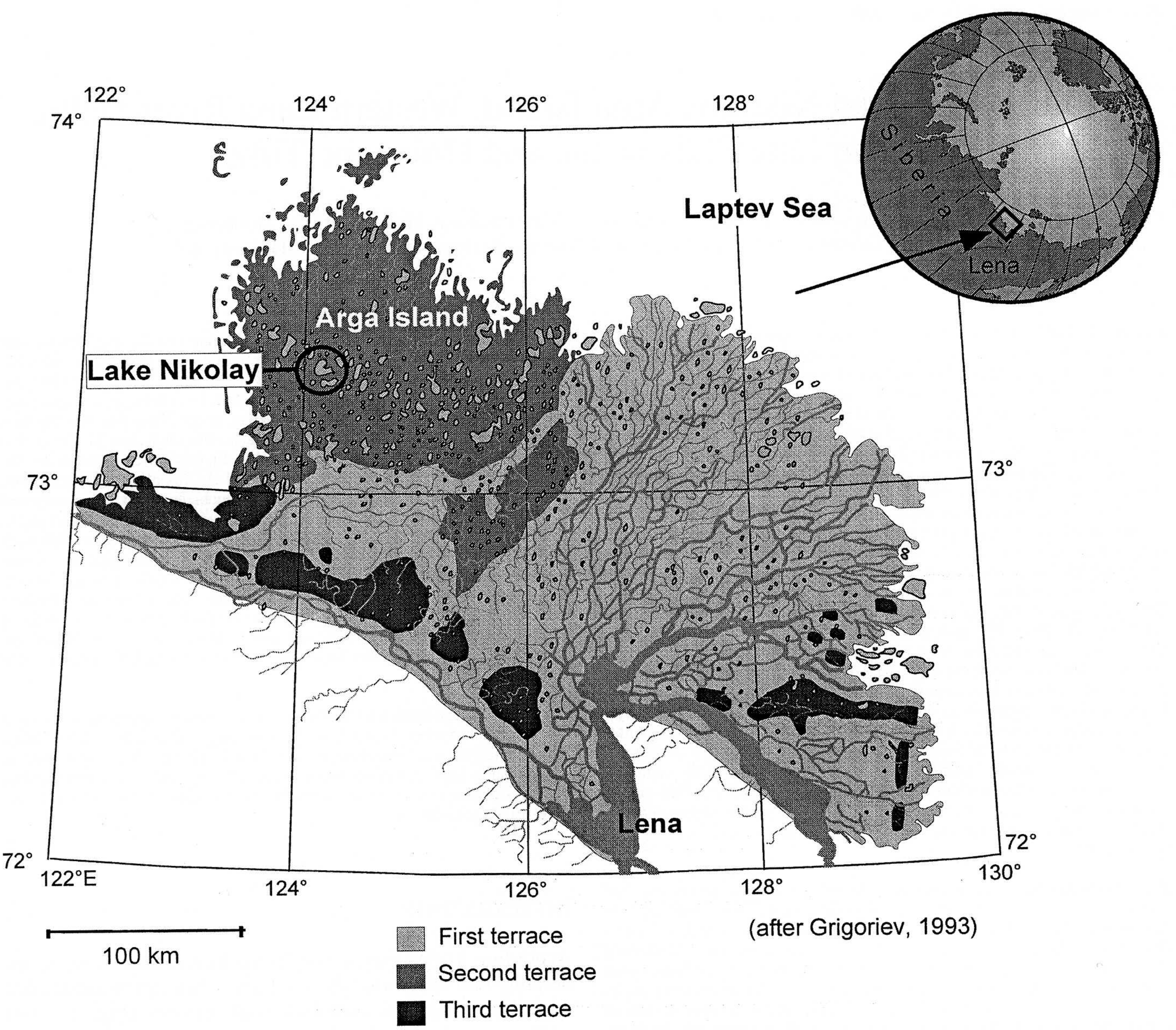

Fig. 1: Location of the study site Lake Nikolay. The lake is positioned on Arga Island, which represents the major part of the second terrace in the Lena River delta.

Abb. 1: Das Untersuchungsgebiet im westlichen Lena-Delta. Der Nikolay-See befindet sich auf der Arga-Insel, die den größten Teil der zweiten Terrasse aufbaut.

favors a panarctic ice sheet covering the entire Arctic continental margin during the last glaciation cycle (GROSSWALD & HUGHES 1999) whereas another viewpoint regards the Eurasian continental margin as partially ice-free during that time (GALABALA 1997). Deposits forming Arga Island developed in a distance to the perimeter of a northern ice sheet.

Arga Island, 110 km in diameter, consists of well-sorted quartz sands and ice wedges penetrating the sandy sediments are abundant. The Arga deposits are presumably of fluvial origin (GRIGORIEV 1993). However, several authors have considered other processes to explain their genesis, i.e. a marine or lagoonal derivation, a limnic-alluvial or an alluvial-aeolian origin (GRIGORIEV et al. 2000 and various authors cited therein). The sedimentary environment is attributed to an intracontinental or half-open basin partly connected to the sea. From the glacial viewpoint ice-rich frozen sands and silts are suggested that accumulated in meltwater paleo-basins confined by a proximal marine ice sheet from the north (GROSSWALD 1998). Meltwater streams may even have tunneled under the grounding line of the panarctic ice shelf (GROSSWALD & HUGHES 1999). The periglacial viewpoint expressively excludes oscillations of the shelf ice sheet onto land and regards the sandy accumulations as outwash plains derived from local snow glaciers located in the mountainous areas on continental Siberia at the relevant time (GALABALA 1997). This also includes a considerable amount of aeolian accumulation (Fig. 2).

Upon these sandy sediments a lake relief developed in the centrally positioned watershed of the island. The long axis of most of the lakes shows a submeridional orientation typifying

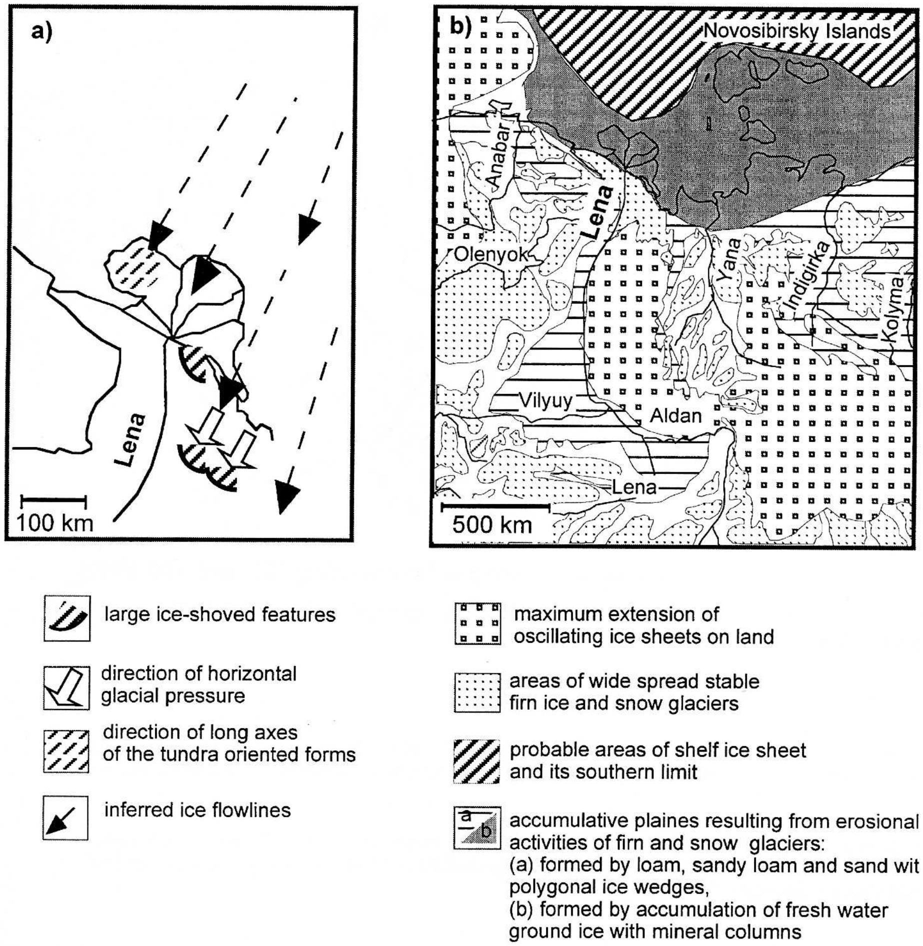

Fig. 2: There are two main hypotheses upon the origin of the sandy deposits and the lake area placed in the western Lena River delta: a glacial (a) and a periglacial (b). Map a) points to the geomorphological complexes of the north Yakutian lowland and adjacent areas simplified according to GROSSWALD (1998) and GROSSWALD et al. (1999). (b) shows the paleogeographical sketch-map of the Weichselian Glaciation in Northern Siberia according to GALABALA (1997).

Abb. 2: Hauptthesen zur Genese der sandigen Ablagerungen und der Seenlandschaft im westlichen Lena-Delta: (a) glazial, (b) periglazial (b). Karte a) verweist auf die geomorphologischen Komplexe im nordjakutischen Tiefland und angrenzender Gebiete vereinfacht nach GROSSWALD (1998) und GROSSWALD et al. (1999). Karte b) zeigt die paläogeographische Vorstellung der weichselzeitlichen Vereisung in Nord-Sibirien nach GALABALA (1997).

lake depressions of elliptical shape. The maximum water depth is in the range of 10-30 m for most of the lakes (GRIGORIEV 1993). These deep lake basins are surrounded by shallow submerged rims (up to 1 km wide) with water depths of less than 2 m. Often two or three basins merge to create a composite lake. Local subsidence may create minor depressions in the shallow lake areas. Lake Nikolay shows this typical form and bathymetry (Fig. 3a).

The central lake basins are believed to be either fluvial or lagoonal or deflation depressions that have been modified by aeolian and cryogenic processes as discussed in GRIGORIEV et al. (2000 and citations therein). Another suggestion relies on the assumption that the lake relief on Arga Island is a typical lake-thermokarst relief. A thawing of excess ice bodies in the subground is postulated in order to explain the thaw settlement below the lake basins, even though discrete ice bodies have not been detected yet (ARE & REIMNITZ 2000). In contrast, the glacial viewpoint explains the lake basins as erosion forms connected with glacial furrows (GROSSWALD et al. 1999).

The main objective of this study is directed to this controversy whereby determining the age and genesis of Lake Nikolay, which is the largest amongst the lakes on Arga Island. Therefore, it might mirror large parts of the history of Arga Island. The lake is up to 8 km wide from west to east and up to 6 km long from north to south. It consists of five sub-basins but approximately 70 % of the lake area have a water depth of less than 2 m. In the shallow parts, below a thin (0.5 m) active layer, the underlying sediments are perennially frozen. Radiocarbon and IR-OSL age determinations and sedimentological studies (ice water content, granulometry, organic carbon content) are applied to reconstruct sedimentation processes and environmental conditions during the deposition of both lake and permafrost sediments. Geophysical profiling is used to obtain subsurface information of the lake basin (Fig. 3b).

METHODS

Fieldwork and sampling was carried out during the expeditions LENA 1998 (RACHOLD & GRIGORIEV 1999) and LENA 1999 (RACHOLD & GRIGORIEV 2000). Geophysical surveys and sediment sampling have been performed for both lake and permafrost deposits. In addition, mathematical modeling has been applied to aid geophysical data interpretation.

Geophysical profiling

A survey of shallow seismic and radio-echo sounding (RES) was run to explore the mosaique of limnic and cryo-terrigenic environments (Fig. 3b). Seismic studies concentrated on the deeper parts of the lake where the water depths range from 10 to 30 m (the greatest depth in one of the sub-basins). A sediment echo sounder (GeoChirp 6100A, Geoacoustics, UK) with high-frequency pulse of 1.5-11.5 kHz installed aboard a rubber boat was used for surveying the deeper lake basins. It

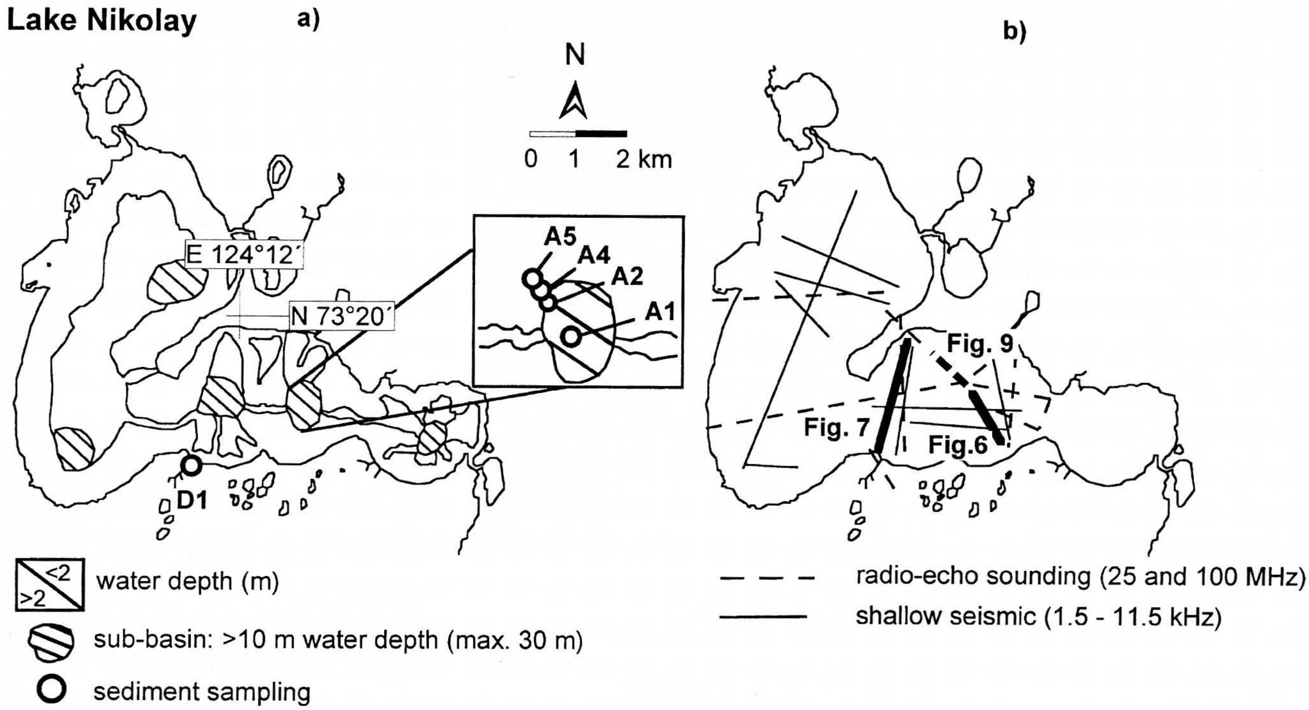

Fig. 3: Lake Nikolay; (a) bathymetry and sediment sampling sites (box). Sub-basins and shallow margins are delined as measured by a portable infrared sounder aboard a rubber boat and with the aid of aerial photography. (b) shows the positions of geophysical profiles. Profiles described in the text are shown in bold lines; Figure numbers are indicated.

Abb. 3: Nikolay-See. (a) Bathymetrie und Probenahmepunkte (Kasten). Teilbecken und flache Uferbereiche ausgewiesen nach Messungen mit tragbarer Infrarot-Sonde an Bord eines Schlauchbootes und Verwendung von Luftbildern. (b) Lage der geophysikalischen Profile. Die im Text erwähnten Profile sind fett hervorgehoben und mit ihren Abbildungs-Nummern gekennzeichnet.

allows a theoretical vertical resolution of ca. 35 cm (QUINN 1997) of the processed chirp data. Recording time of the GeoChirp is restricted to a time window of 130 ms TWT (two-way travel time). The seismic reflections are automatically processed during the cruises applying a cross-correlation and analogue print-outs are provided already in the field. These prints are used for presentation in this paper. An approximation of penetration depth is based on assuming average sonic velocities of 1420 m/s for water and 1490 m/s for unconsolidated limnic sediments (NIESSEN & MELLES 1995) and 1800 m/s for compressed sandy sediments (EYLES & MULLINS 1997, NIESSEN & JARRARD 1998).

RES studies allowed extending the subsurface profiling to the marginal parts of the lake where wave penetration into the permafrost was possible by electromagnetic (EM) means. Profiling has been carried out using 25 and 100 MHz antenna pairs from the winter ice cover in connection with drilling activities. RES is an established technique for permafrost investigations (ANNAN & DAVIES 1976, JUDGE et al. 1991, ROBINSON et al. 1997) and the potential of this method for surveying lake sediments through an ice cover has been documented (MOORMAN & MICHEL 1997).

A RAMAC impulse radar system (Mala/Geoscience) was used for RES profiling. In order to determine the velocity-depth function of the EM waves, common mid-point (CMP) measurements were recorded at characteristic sites like shallow lake areas, deep basins and on land. To verify the CMP measurements the thickness of the lake ice and the water depths were measured in the field with a plumb line and a measuring tape. During the summer surveys on land in August 1998 the thickness of the active layer was determined.

The propagation velocities for the EM waves were measured 55 m/µs for saturated lake sediments, 161 m/µs for permafrost below the lake ice and 173 m/µs for lake ice. The value for water is set to 33 m/µs according to DAVIES & ANNAN (1989). Estimates of depths in different media are based on these values. As the resolution of RES is dependent on the wavelength in the different media (MOORMAN & MICHEL 1997) the approximate vertical resolution for example with the 100 MHz antenna pair was calculated in the permafrost 0.7 m and in the water-saturated lake sediments 0.3 m, respectively. In total, 13 profiles were collected with data for about 25 km of lake sediments. The field survey was operated by a computer and the resulting reflections were on-line visualized on the screen. Lab processing of the radar sections included time-zero correction, band-pass filtering, automatic gain control and corrections for topographic migration wherever necessary.

During the field work RES was used to determine appropriate lake sediment coring sites. Vice versa, the core data are used to interpret the reflection pattern of the radargrams.

Sediment sampling

A drilling transect was undertaken to obtain continuous core samples from one of Lake Nikolay's sub-basins to the shallow margin around it. The sampling sites (cores A1, A2, A4 and A5) are displayed in Figure 3a. Vertical drilling in both frozen and unfrozen lake sediments was performed from the ice using a frozen-ground rotary coring kit consisting of an engine power-auger unit, iron rods, and iron core barrels. Samples of second terrace deposits around the lake have been retrieved by drilling into the permafrost at a manually cleaned outcrop near the shore. A HILTI drilling machine was used to recover frozen samples horizontally out of a 5 m sandy sequence (sampling site D1).

Core sections were cleaned, described and stored immediately after sectioning. By packaging each individual sample in the field, it was unnecessary to maintain the samples in their frozen state during transit to the laboratory.

Laboratory methods

After the sediment samples had been examined for moisture (gravimetric water content) the grain-size distribution was determined by laser particle sizing (LS200, Coulter Corp.) for both core and outcrop sediments. Individual samples were oxidized (3 % H_2O_2) to remove organic matter and dispersed (10 % NH_4OH) to diminish surface tension. Total organic carbon (TOC) was analyzed with a Metalyt-CS-1000-S (Eltra Corp.) on pulverized samples after removal of carbonate (10 % HCl) at a temperature of 80 °C. International standard reference materials (GSD, 9, 10, 11) as well as double measurements were used to check the external precision. The analytical precision of the analyses is ±5 % for TOC contents >1 wt% and ±10 % for TOC contents <1 wt%.

A stable carbon isotope profile was determined for organic material of core A1 from the basin center. $^{13}C/^{12}C$ isotope ratios were measured using a FINNIGAN DELTA S mass spectrometer after removal of carbonate with 1 N HCl in Ag-cups and combustion to CO_2 in a Heraeus elemental analyzer (FRY et al. 1992). Accuracy of the analytical methods was checked by parallel analysis of international standard reference material. The analytical precision of the carbon isotope analyses is ± 0.2 ‰.

Finally, the pollen record of core A1 was analyzed. Pollen samples were prepared using standard techniques (FØGRI & IVERSEN 1989). For each sample 200-300 terrestrial pollen grains were counted at 400 times magnification. Spores were counted in addition and the relative frequency of pollen, spores and algae was determined according to BERGLUND & RALSKA-JASIVECZOWA (1986). Selected organic-rich layers and plant remains were used for AMS radiocarbon dating at the Leibniz Laboratory, Kiel. Radiocarbon ages (^{14}C yr BP) were calibrated into calendar years before present (cal. yr B.P.) according to the intercept method (STUIVER et al. 1998).

Mathematical modelling

In one seismic profile a prominent reflector is interpreted to show the boundary between frozen and unfrozen sediment below one of the sub-basins. To test this hypothesis a mathematical model has been calculated illustrating the thawing propagation. The two-dimensional axisymmetrical model used takes into account cryolithogenic properties and lake evolution in time. The equation for heat conduction is described by a finite differences method. For simulation the computational area was set to a size of 3600 m in horizontal and 3000 m in vertical direction. The initial distribution of temperatures was determined according to the boundary conditions. They are based on measured field data (water temperature, depth, permafrost temperature according to SCHWAMBORN et al. 2000b) and include the age of the lake (SCHWAMBORN et al. 2000a). The thawing development below the deeper basin only has been estimated excluding the shallow-water margin around the basin. The following presumptions are made:

(1) Lake Nikolay predominantly has a thermokarst genesis, i.e. it has developed due to the thawing of frozen deposits that have a thickness of at least 10 m and a volumetric ice content of 25 %.

(2) Lake formation started at 7000 ^{14}C yr BP.

(3) The occurrence of massive ice bodies is excluded and, thus, does not affect subsidence.

(4) The thermophysical properties of the deposits at Lake Nikolay that could not be determined are similar to those of sand deposits in the north of Western Siberia (ERSHOV 1984). They have a comparable genesis, grain size and moisture (ice content). Since these parameters are changeable, they are reviewed in versions of different groups (N1 through 3) of thermophysical properties (Tab. 1).

(5) The geothermal heat flux at the lower boundary is 50 mW/m^2 and the dynamics of mean annual ground temperature are according to Vostok ice core data from Antarctica (PETIT et al. 1999), which have been customized for the Laptev Sea region (GAVRILOV et al. 2000).

RESULTS AND DISCUSSION

Land deposits

An outcrop near the southern lake shore exposes about 5 m of fine-grained sand belonging to the second terrace of the Lena River delta (site D1 in Fig. 3a). The sand is bound by lense-shaped texture ice and contains a complex system of narrow ice veins. It is noteworthy that the geomorphic situation at the southern shore banks, where site D1 is located, is more stable than at the northern ones. Thermoabrasion is active around the entire lake, but especially along its northern margin. Due to the high latitudinal position of the area insolation is higher at southerly exposed slopes. Destruction and retreat of the northern shore banks is more rapid, therefore supporting a lake elongation towards the north. For Lake Nikolay this relationship - insolation effects and bank retreat - is favoured against a predominance of wave (wind) action influencing the lake's shape as preferred in a review of literature on the elongation of oriented thaw lakes in periglacial regions by FRENCH (1996).

The sediments as found at the bluffs around Lake Nikolay are lacking pronounced bedding structures and appear as massive fine-sandy accumulations. Throughout the sequence of site D1 the sediments show similar grain size distributions with mean grain sizes varying between 2.0 and 2.5 phi (1st statistical moment). They are well to moderately sorted (2nd statistical moment: 0.8-1.4) and poor in organic content (TOC content ≤ 0.1 wt%). Gravimetric ice content of the frozen sands does not

	groups	λ_f	λ_t	C_f	C_t	Q	γ	W
Common data for West Siberia, fine sand, laIII-IV	N 1	2.2	2.16	1920	2630	113970	1700	0.2
Common data for West Siberia, dusty sand, laIII-IV	N2	1.82	1.46	1920	2630	113970	1700	0.2
Middle part of Ob' River dusty fine sand, laII	N3	2.05	1.99	1860	2520	106995	1680	0.19

Tab. 1: Thermal properties of deposits adopted for the simulation according to ERSHOV (1984) and GAVRILOV et al. (2000). Three groups of Siberian sandy deposits (N1-N3) have been defined.
λ_f = frozen thermal conductivity, [W/(m*K)]; λ_t = unfrozen thermal conductivity, [W/(m*K)]; C_f = frozen heat capacity, [J/m^3*K]; C_t = unfrozen heat capacity, [J/m^3*K]; Q = latent heat [J/m^3]; γ = density [kg/m^3]; W = sand moisture.

Tab. 1: Thermale Eigenschaften der Ablagerungen, die für die Modellierung herangezogen werden; nach ERSHOV (1984) und GAVRILOV et al. (2000). Es werden drei Gruppen sandiger Ablagerungen Sibiriens unterschieden (N1-N3).

exceed 20 wt%. The ice veins, up to 0.5 m wide, build up ice wedge polygons of 10-15 m diameter towards the surface. Formation of the ice wedges is probably of Late Pleistocene to Early Holocene age as deduced from oxygen isotope measurements (H. MEYER unpubl. data). The results resemble measurements from Bykovsky Peninsula, southeast of the Lena River delta, which have been dated accordingly (MEYER et al. 2002). Downwards the fabric of ice veins can reach depths of 50 m and more as indicated by RES records (SCHWAMBORN et al. 2000c). Luminescence datings, which were conducted to the sandy sequence, reveal a time span of deposition from 14,500-10,900 yr BP (KRBETSCHEK et al. 2002). Since the post Pleistocene transgression of the Laptev Sea only reached its modern coastline at about 6000-5000 yr BP (HOLMES & CREAGER 1974, BAUCH et al. 1999, ROMANOVSKII et al. 1999), the sediments of Arga Island have to be related to a continental environment. The high sedimentation rate implied by the overlapping ranges of the luminescence ages probably is associated with a fluvial environment under upper flow regime. It has been shown at comparable river bed sediments of the Russian Plain and of the same age that periglacial river channels during and posterior to the Weichselian Glaciation were formed under conditions of high water flow during spring that is believed to have been up to eight times greater than the modern discharges (PANIN et al. 1999, SIDORCHUK et al. 2000). Correspondingly, marine records from the outer Laptev Shelf have revealed that significant climate changes at the termination of the Pleistocene led to rapid increases of sediment supply to the Arctic Ocean after 15,000 and 13,000 yr BP (MÜLLER & STEIN 2000, BOUCSEIN et al. 2000, SPIELHAGEN et al. 1998). This is supported by seismic penetration into pre-Holocene paleoriver channels identified on the Laptev Sea shelf in Parasound profiles (KLEIBER & NIESSEN 2000). The seismic records and drilling results suggest that the river runoff was continuous through the major valleys on the exposed Laptev Shelf with increased input between approximately 13,400 and 10,000 yr BP. Furthermore, these events seem to coincide with abrupt changes in the hydrological and environmental conditions in the non-glaciated continental lowland areas of Siberia. Numerous permafrost sites show evidence for a rapid increase of denudation linked with activation of different geocryological (solifluction, thermokarst, thermal erosion etc.) and fluvial processes during this time (SIEGERT 1999). For example, the formation of the deep and wide valleys of tributaries of the middle Lena River were dated to have occurred before 14,000 yr BP (KATASONOVA & ZIEGERT 1982). Pronounced thermokarst processes started at 13,000 yr BP, for example on glacial deposits with dead-ice bodies in the Labaz Lake area (Taymyr Peninsula) (SIEGERT et al. 1999) and at Ice Complexes in the central Yakutian lowland (KATASONOV et al. 1999). In general, the north Yakutian lowlands are thought to have remained ice-free for the last 50,000 yr BP (ROMANOVSKII et al. 2000). Massive bodies of Ice Complexes in the area, as on Bykovsky Peninsula, have preserved a continuous record of environmental history from the Early Weichselian to Holocene time (SCHIRRMEISTER et al. 2000, SIEGERT et al. 2002). These climate-induced formations can only form in non-glaciated environments.

Summarized, a periglacial and continental environment is proposed for Arga Island during Late Pleistocene time. Seasonally dependent river activity with higher peak discharges led to high sediment transport and deposition of thick fluvial sequences in the North Yakutian lowlands. Partially they are preserved in morphological terraces like Arga Island north of the continental mountains or distributed along river valleys on the Siberian mainland as shown by GALABALA (1997).

Lake sediment stratigraphy

Lake basin sediments were sampled in the middle of one subbasin (core A1) of Lake Nikolay, where sedimentation is not affected by marginal gravitational sliding. Core A1 has been recovered in a length of 3.25 m. Based on field description and according to physical and biogeochemical measurements the core can be divided into two sedimentary units (Fig. 4). The upper unit (0.9 m) consists of organic-rich fine sand (max. TOC content: 3.9 wt%, water content: 30-60 wt%) with sporadical plant fragments. This unit is regarded as lake sediment reaching from the modern status backwards in time. The lower unit of the core (2.35 m) consists of fine sand. The sands of this unit are interpreted to have the same origin as the sediments at the bluffs around the lake. The structureless sandy sediments of the lower unit from core A1 match the sandy deposits of site D1 in terms of similar mean grain sizes (1st statistical moment: 2.4-3.4 phi), sorting (2nd statistical moment: 1.3-2.1), low TOC content (<0.1) and water content (<20 wt%).

When comparing the grain size characteristics of the lower and the upper unit of core A1 both core units show a narrow range of grain size (Fig. 4). Yet, a shift in the median by ~64 µm from coarser grains in the lower unit to finer grains in the upper unit can be seen. This is interpreted as resulting from a considerable aeolian contribution to the sedimentation of the upper unit. In the modern lake sediments sand derived from aeolian transport admixes with presumably suspended material from the small inlets around the lake. This may lead to a slight decrease in mean grain size due to a preferential transport of sand with smaller grain sizes. The incomplete vegetation cover in the area and exposed ground would have allowed considerable transport of silty sand by wind. Strong winter winds are capable to expose bare ground and move sandy dust across the surface, as seen on the lake ice and on land during our field work. Holocene aeolian sediments are widely spread on Arga Island. They consist of silty sand with vertical plant stems and roots (GALABALA 1997).

Four AMS ^{14}C dates in a consistent depth/time relation were obtained from plant remains revealing a maximum age of about 7090 ±40 ^{14}C yr BP (Tab. 2) for the upper unit. This age marks the beginning of organic-rich sedimentation in the depression. The oldest date of 12,480 ±60 ^{14}C yr BP dates presumed pre-lake material of the lower unit. This age agrees well with the IR-OSL ages of 14,500-10,900 yr BP measured for the sandy sediments at site D1.

Organic carbon record

The organic carbon isotope record ($\delta^{13}C_{org.}$) of the lake sediments includes 21 samples of bulk organic material of the upper unit from core A1. The low TOC values for the underlying pre-lake sediments show that organic matter plays a negligible role (Fig. 4). Organic-rich sediments of the upper unit have been deposited with a narrow range of $\delta^{13}C_{org.}$ values between -25 and -27 ‰ V-PDB. This is similar to $\delta^{13}C_{org.}$ values from -26.6 to -24.3 ‰ V-PDB of terrestrial plant material in this climatic region (GUNDELWEIN 1998). In contrast, fresh-water plankton generally has depleted $\delta^{13}C_{org.}$ values of -30.0 ±3 ‰ V-PDB (ARIZTEGUI & MCKENZIE 1995). Modern autochthonous macrophytes of Lake Nikolay fall between these two ranges with values of -26.3 ‰ V-PDB. A negative

No.	Core depth (m)	Lab. No.	measured age (^{14}C yr BP)	calibrated age (cal, yr B.P.)
A1	0.1	KIA9113	2080±30	2060
A1	0.3	KIA9114	4335±40	4910
A1	0.85	KIA9115	7090±40	7920
A1	0.95	KIA9116	12480±60	14850

Tab. 2: AMS radiocarbon ages and calculated calendar years for core A1.

Tab. 2: AMS-Radiokarbonalter und berechnete Kalenderjahre für den Sedimentkern A1.

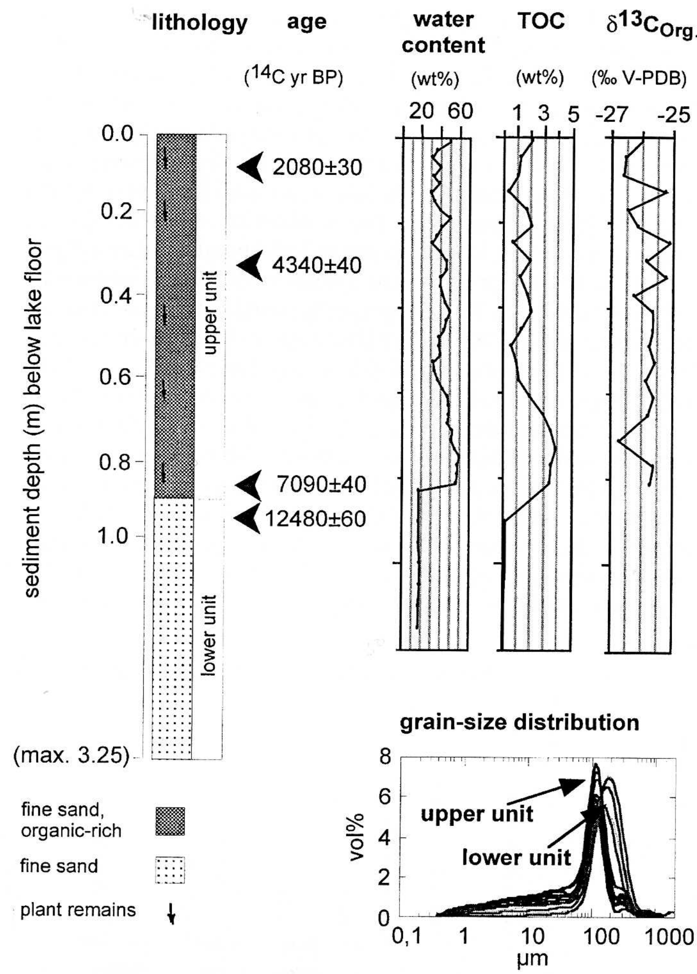

Fig. 4: Sediment profile of one lake basin (Core A1) showing ^{14}C ages, water content, total organic carbon (TOC), organic carbon isotopes and grain-size distributions.

Abb. 4: Sedimentprofil des Seebecken-Kerns A1 mit ^{14}C-Altern, Wassergehalten, gesamtem organischen Kohlenstoff (TOC), C-Isotopen des organischen Kohlenstoffs und Korngrößenverteilungen.

correlation between TOC concentrations and the $\delta^{13}C_{org.}$ values in the upper unit is seen in Figure 4. A prominent maximum in the TOC content at about 7000-6000 ^{14}C yr BP and a few minor TOC maxima following towards the top of the section are paralleled by shifts of $\delta^{13}C_{org.}$ towards lighter values. These findings indicate that lighter $\delta^{13}C_{org.}$ values can be explained by an increasing contribution from plankton. Thus, light $\delta^{13}C_{org.}$ values indicate high lake-internal productivity and correlation with high TOC values mirrors lake production for Lake Nikolay rather than terrestrial supply. It confirms the suggestion of little supply from the catchment made by the grain size data. The generally rather small range of carbon isotopes indicates that the lake environment seemed environmentally stable at least after the bioproductive maximum between 7000-6000 ^{14}C yr BP.

Vegetation history

Also the pollen spectra of core A1 provide information about paleoenvironmental changes over the last 12,500 ^{14}C yr (Fig.

5). A high percentage of algae (*Pediastrum* and *Botryococcus*) occur in the lower unit of the core radiocarbon dated at 12,480 ±60 ^{14}C yr BP. This is associated with a shallow water environment, for example a water pond, at that time. Pollen data reflect that scarce sedge and grass dominated the vegetation with some *Artemisia* communities on dryer ground. Rare grains of *Alnus fruticosa, Betula nana* and *Salix* may reflect the reworked character of the sediments, or these species might have grown in well-protected places of the Lena River valley. Very few pollen were found in the sandy sediments between 0.9-1.0 m. Pollen spectra deposited at the onset of the upper unit about 7000 ^{14}C yr BP suggest that shrubby vegetation *(Alnus fruticosa* and *Betula nana)* dominated around the lake. High amounts of *Cyperaceae*, *Ericales* pollen, *Equisetum* spores and the presence of *Menyanthes trifoliata* pollen indicate wide distribution of wetlands. Shrubby tundra with shrub alder *(Alnus fruticosa)* and dwarf birch *(Betula nana)* dominated around the lake from 7000 to 6000 ^{14}C yr BP. This requires that climate was significantly warmer then today. Other pollen and plant macrofossil data from the area also support that the warmest climate occurred during that time (MACDONALD et al. 2000, ANDREEV et al. 2001, PISARIC et al. 2001, ANDREEV et al. 2002). The pollen concentration is highest, reflecting high productivity of plant communities on Arga Island. These data are in a good agreement with a TOC maximum between 7000-6000 ^{14}C yr BP in the lake sediments (Fig. 4). Between 6000-5000 ^{14}C yr BP a decrease of *Alnus fruticosa* and *Betula nana* pollen and a significant increase of long-distance transported pollen of *Picea obovata*, *Pinus pumila* and *P. sylvestris* document changes in the local vegetation and a decrease in productivity of the plant communities. Such deterioration of climatic conditions is probably connected with the sea-level rise to its present level about 6000-5000 yr BP (BAUCH et al. 1999). The climate after that time in many coastal Arctic regions became more maritime (ANDREEV & KLIMANOV 2000). Shrub alder communities were probably growing on the island during that time. Disappearance of *Alnus* from pollen spectra after 4300-4200 ^{14}C yr BP is in a good agreement with pollen data from Bykovsky Peninsula, southeast of the Lena River delta, where *Alnus fruticosa* pollen also declined about that time (ANDREEV et al. 2002). It is interesting to note that the youngest *Larix* remains

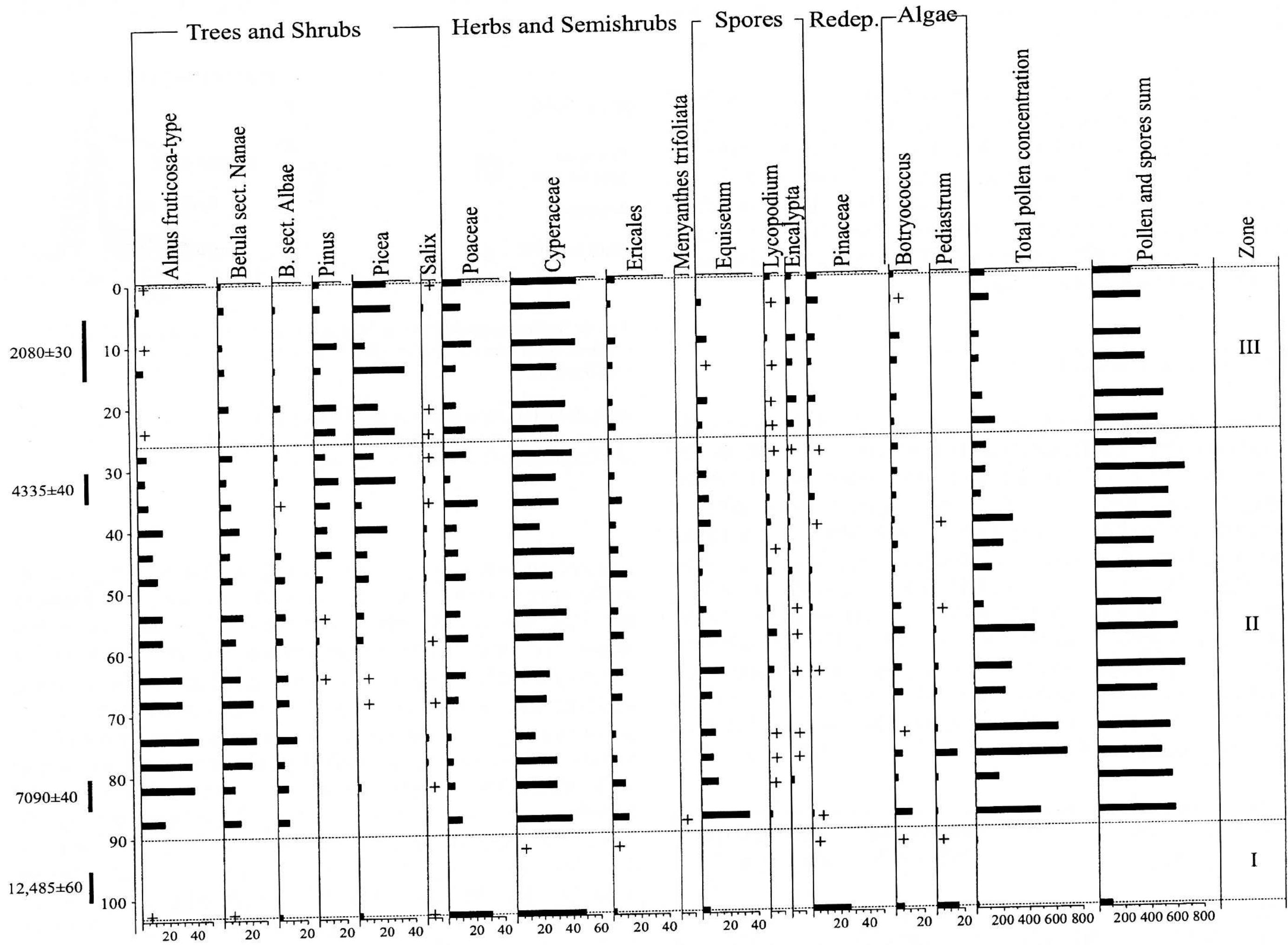

Fig. 5: Pollen spectra of core A1. The determination of the relative frequency of pollen is based on the sum of tree and herbs pollen. The percentage of spores is based on the sum of pollen and spores. The percentage of redeposited taxa (Tertiary spores and Pinaceae) is based on the sum of pollen and redeposited taxa. The percentage of algae is based on the sum of pollen and algae.

Abb. 5: Pollenspektren des Kerns A1. Die Bestimmung der relativen Pollenhäufigkeit basiert auf der Summe der Baum- und Kräuterpollen. Der prozentuale Anteil an Sporen basiert auf der Summe von Pollen und Sporen. Der prozentuale Anteil umgelagerter Taxa (tertiäre Sporen und Pinaceae) basiert auf der Summe von Pollen und umgelagerter Taxa. Der Prozentsatz an Algen basiert auf der Summe von Pollen und Algen.

found above the modern treeline (Tit-Ary Island area) are also dated at 4200 ^{14}C yr BP (MACDONALD et al. 2000). Pollen data suggest that climate during that period was the most favorable for the terrestrial and limnic ecosystems. Pollen spectra dated at 4000-2000 ^{14}C yr BP reflect that herb-shrubby tundra with dwarf birch (*Betula nana*) dominated around the lake during this period. Relatively high amounts of reworked Pinaceae pollen and *Encalypta* spores (moss growing on disturbed soils) reflect scarce vegetation cover during that time.

Vegetation cover and climate became similar to modern conditions at about 2000 ^{14}C yr BP. Open sedge and grass communities have been dominating in the area since then. The high percentages of long distance transported pollen such as *Picea* and *Pinus* reflect low pollen productivity of local plant communities.

Seismic stratigraphy of basin fills

As has been shown Lake Nikolay is dominated by sandy sediments. The basin fill covers different subaqueous relief levels and varies in thickness in the decimeter to meter range (SCHWAMBORN et al. 1999). Based on the geometry of subbottom profile shown in Figure 6 three seismic units can be identified. They are referred to as seismic units (SU) 1 through 3.

SU 1: The uppermost boundary shows continuous to semicontinuous reflections of laterally alternating high and low amplitudes. Changing backscatter of the reflectors may be due to variations of organic matter content in the sediments, which at site A1 mainly consist of organic-rich fine sand as seen in the core. The first reflections of SU 1 are underlain by a narrow band, which is seismically transparent. The total thickness of both parts of this unit amounts to 0.5-1.0 m. SU 1 continuously overlies the underlying units. The draping of SU 2 by SU 1 without large differences in SU1 thicknesses indicates sedimentation from "pelagic" rain. This suspensional transport through the water column may be promoted by the small inflows shown in Figure 3a and aeolian sediment supply as mentioned earlier.

SU 2: The top of SU 2 is marked by a strong continuous reflector. Below this the unit alternates from transparent parts to parts with several internal reflectors. The unit locally thins to decimeters and pinches out in the central parts of the basin, but thickens to as much as 5 m at the margin. It suggests that slumping or turbidity currents will have caused the observed geometry. Core A1 indicates the lithofacies of this unit as fine sand in the relevant part of the core. The water content changes sharply from 30-60 wt% in the upper part of the core to about 20 wt% in the lower part, which is relevant to SU 2. This contrast in water content is interpreted to have caused the uppermost reflections of SU 2.

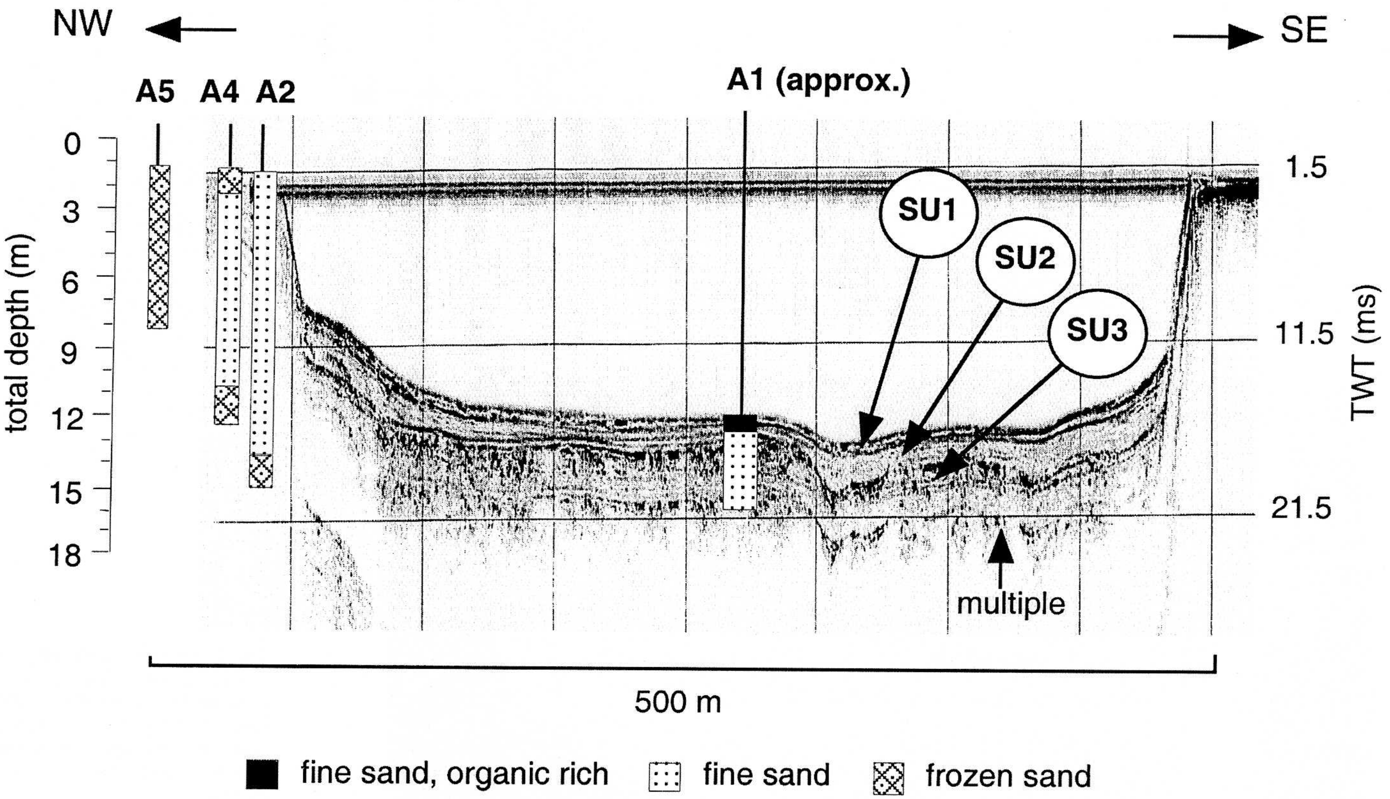

Fig. 6: Shallow seismic profile illustrating the acoustic stratigraphy of the studied basin sediments (VE : ~1:5). For interpretations of the seismic units 1 through 3 (SU 1-3) see the text. Approximate locations of sampling sites A1, A2, A4 and A5 are indicated.

Abb. 6: Flachseismisches Profil, das die akustische Stratigraphie der untersuchten Beckensedimente illustriert. Siehe Text zur Interpretation der seismischen Einheiten 1 bis 3 (SU 1-3). Lokalitäten der Bohrstellen A1, A2, A4 und A5 sind markiert.

SU 3: The upper surface of SU 3 varies from smooth to hummocky. Below a strong upper reflector internal reflectors are horizontally stratified or spotty. The causes of the internal reflectors of SU 3 remain unclear since the core A1 does not provide a clear indication. It consists of fine sand only in the relevant part of the core as already described for SU 2. Unfortunately, a multiple of the upper surface of SU 3 occurs in the seismic data. This interferes with further stratigraphic interpretations and a lower boundary of SU 3 is not clearly visible. Either wave penetration has ceased due to loss of energy or the restriction of the GeoChirp´s time window prevents more subbottom detail. Assuming the same material below the lake as around it, as indicated by sediment data from core A1 and site D1, the subground of Lake Nikolay consists of massive fine sand down to at least 60 m sediment depth. This is suggested by RES measurements around site D1, which show a continuous radar facies pointing to a uniform geological substrate of this thickness (SCHWAMBORN et al. 2000c).

Talik development

Seismic indication of talik contours

One of the seismic profiles penetrates as much as 120 ms TWT and reveals a curved reflector below one of the sub-basins (Fig. 7). This reflector corresponds to about 95 m of fill at maximum below the water column. With a steep drop in the beginning of the profile, the unit thickens to about 110 ms TWT in the southern part of the basin. It then thins slightly towards the northern part of the profile before abruptly pinching out. In contrast to layered seismic reflections, which are generally indicative of sediment changes, the trough-like curved seismic boundary is assumed to be created by the talik-permafrost boundary. Outside of the talik outline seismic penetration is prevented by the permafrost table and sediment structures within the permafrost remain unknown. The lack of internal reflectors for the recorded talik area suggests that the

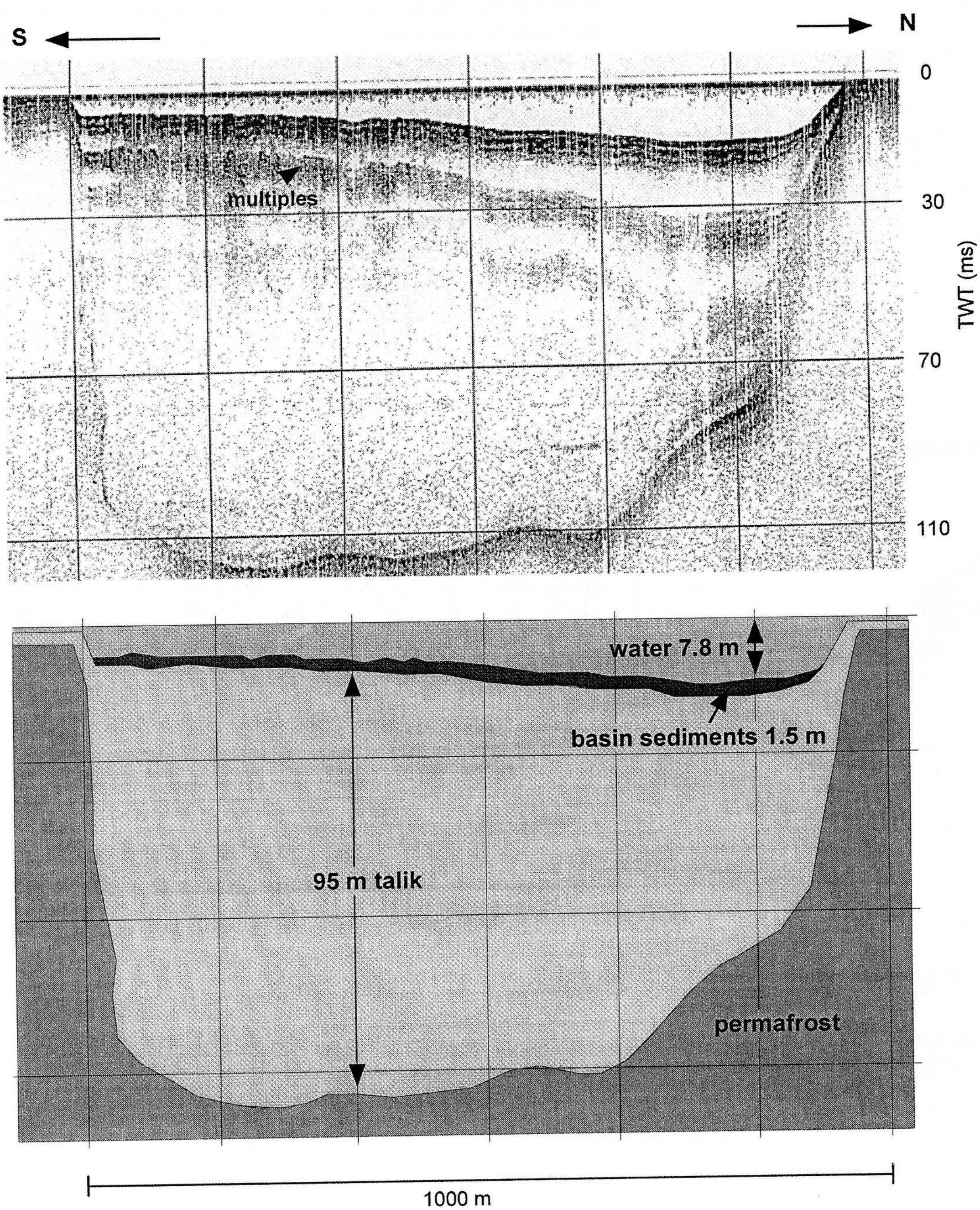

Fig. 7: Shallow seismic prof exhibiting a prominent curv reflector below one of the su basins (VE: ~1:5). This repr sents the boundary betwe unfrozen and frozen sec ments.

Abb. 7: Seismisches Profil r deutlichem, gekrümmtem R flektor unter einem der Te becken (vertikale Überhöhur ~1:5). Der Reflektor wird Grenze zwischen aufgetaute und gefrorenem Sediment terpretiert.

acoustic waves have penetrated a fairly homogenous substrate with little internal sedimentary structure and/or low acoustic contrasts, respectively. Possible sedimentary changes may be too subtle to be resolved. An additional sedimentary explanation for the acoustic transparency could be the fact that internal layering of talik sediments may have been destroyed due to thaw and subsidence.

On the other hand, the propagation of acoustic energy through the water column and sub-surface generally results in energy loss due to spherical spreading of the wave front, attenuation by inter-granular friction loss and the reflection coefficient of each material interface crossed (SHERIFF & GELDART 1995).

The general lack of internal reflectors, i.e. material interfaces, in the recorded talik means that the attenuation of signal loss is low. Furthermore, multiples caused by the water/lake-sediment interface are weaker than in other profiles. This implies that a greater proportion of the energy may have penetrated the subground, thus enabling the higher penetration. Nevertheless, with increasing penetration depth higher acoustic contrasts are needed to be resolved by seismic means.

To describe the clear reflections presumably caused by the permafrost table below the sub-basin a calculation of the reflection coefficient for this boundary has been applied. Following KEAREY & BROOKS (1984) a reflection coefficient (R) for a deeper reflection can be calculated for seismic data using the following relationship:

$$R = \frac{\rho_2 \nu_2 - \rho_1 \nu_1}{\rho_2 \nu_2 + \rho_1 \nu_1} = \frac{Z_2 - Z_1}{Z_2 + Z_1} \qquad (1)$$

where ρ, ν, Z are the density, the P-wave velocity, the acoustic impedance for an upper (Z_1) and a lower (Z_2) rock layer, respectively. If $R = 0$ all the incident energy is transmitted. This is the case when there is no contrast of acoustic impedance across an interface (i.e. $Z_1 = Z_2$), even if the density and velocity values are different in the two layers. If $R = +1$ or -1, all the incident energy is reflected. Values of reflection coefficient R for interfaces between different rock types rarely exceed ± 0.5 and are typically less than ± 0.2 (KEAREY & BROOKS 1984). There are no field or laboratory measurements available for the fine grained sediments of Lake Nikolay. Therefore, in our case study ν_1 is 1800 m/s as the assumed wave velocity in the fine sandy talik sediments, introduced earlier, ν_2 is 3700 m/s as the wave velocity in unconsolidated permafrost according to measurements on frozen fine sand from the Canadian Arctic (ZIMMERMAN & KING 1986). The latter is a minimum value, seismic velocities in frozen sand can even reach 4190 m/s (ZIMMERMAN & KING 1986). Density values for ν_1 and ν_2 are set to 1.7 g/cm^3 according to measurements on fine sand of deposits in the north of Western Siberia (ERSHOV 1984), which are regarded to be comparable with those of Lake Nikolay. However, frozen sands may have slightly lower density values since the density of ice (0.92 g/cm^3) is lower than that of water.

The result of the calculation of the reflection coefficient for the presumed talik-permafrost boundary is following equation (1) +0.35. The high contrast between the two acoustic impedances allows the boundary to be detected even when there is left only a small amount of seismic energy in greater depth. The differences in the acoustic impedances are mainly caused by their large differences in wave velocities for unfrozen and frozen media.

The permafrost table detected by drilling at one basin margin supports the seismic interpretation. The cryolithogenic properties of sediment cores A2, A4 and A5 next to one lake basin show that the subsurface is unfrozen fine sand (Fig. 6). It only becomes a thoroughly frozen subground at the end of the core transect in a distance of 15-20 m to the basin (core A5). Grain size distributions and ice/water contents of the fine sands from cores A2, A4 and A5 resemble those of the lower unit of core A1.

Results of mathematical modelling

To aid seismic interpretation for the subsurface below the basin a mathematical model has been calculated. It predicts the expansion of a thawing front below the lake basin, where a fresh water body with temperatures above 0 °C induces thawing of surrounding permafrost ground. The model is intended to characterize the cryolithogenic properties of the subground, where no drilling results can provide verification. It is applied to the sub-basin shown in Figure 7. Accepting the initial and boundary conditions and the thermophysical values for the geological material (Tab. 1) the model calculates a talik expansion below the deeper basin as displayed in Figure 8. The calculation initiates at 120,000 yr BP. At 7000 yr BP the lake formation starts and extends to its maximum given size at present with a rate of 2 m/yr. The temperature of the bottom sediments is received to be at first 4 °C, then it decreases down to 2.5 °C in conformity to field data.

We note that the shallow seismic profile does not cover the center of the basin, but is shifted towards its western margin. Thus, the maximum values calculated by the model have to be corrected towards the basin margins assuming that greater water depth in the center of the basin has led to a greater talik depth below it (Tab. 3). The data in Table 3 demonstrate that the talik depth under the lake is dependent mainly on ground heat conduction in thawed and frozen geologic material, respectively. Therefore, the talik depths obtained for groups N1 and N3 describing similar geologic material are similar, for group N2 it is smaller. The average depth of the talik bottom at the basin margin as deduced from the mathematical model is calculated at 106 m. The estimated depth of the curved reflector in the seismic chart is in a good agreement with the calculated talik depth in the model (Fig. 8) and the values of Tab. 3. Consequently, the mathematical model can support the interpretation that the curved seismic reflector represents the boundary between unfrozen and frozen sediment.

Radio-echo sounding of permafrost deposits

RES profiles from the shallow margins of the lake, in contrast to the seismic records, display several internal reflectors in the sediments (Fig. 9). The radar profile of Figure 9 has been recorded as the continuation of seismic profile of Figure 6 towards northwest. The sediments consist of frozen fine sand as seen in core A5. Below the winter lake ice cover (thickness

Distance from basin margin (m)	Bottom depth (m) of the lake talik below lake surface in dependance on the groups N1-N3		
	N1[st] group of thermophys. prop.	N2[nd] group of thermophys prop.	N3[rd] group of thermophys prop.
100	82.8	73.4	81.7
150	116.1	100.4	114.5
200	135.1	115.8	133.7
Central part of sub-basin	159.3	134.3	158.7

Tab. 3: Calculated total bottom depth (m) of lake talik according to the modeling results and in dependance on the distance from the basin margin. Bottom depth (m) of the lake talik below lake surface according to seismic data is ~95 m

Tab. 3: Berechnete Gesamttiefe (m) des See-Taliks entsprechend den Modellierungsergebnissen und in Abhängigkeit von der Beckenrandentfernung. Die Tiefe des See-Taliks nach seismischen Daten beträgt ca. 95 m.

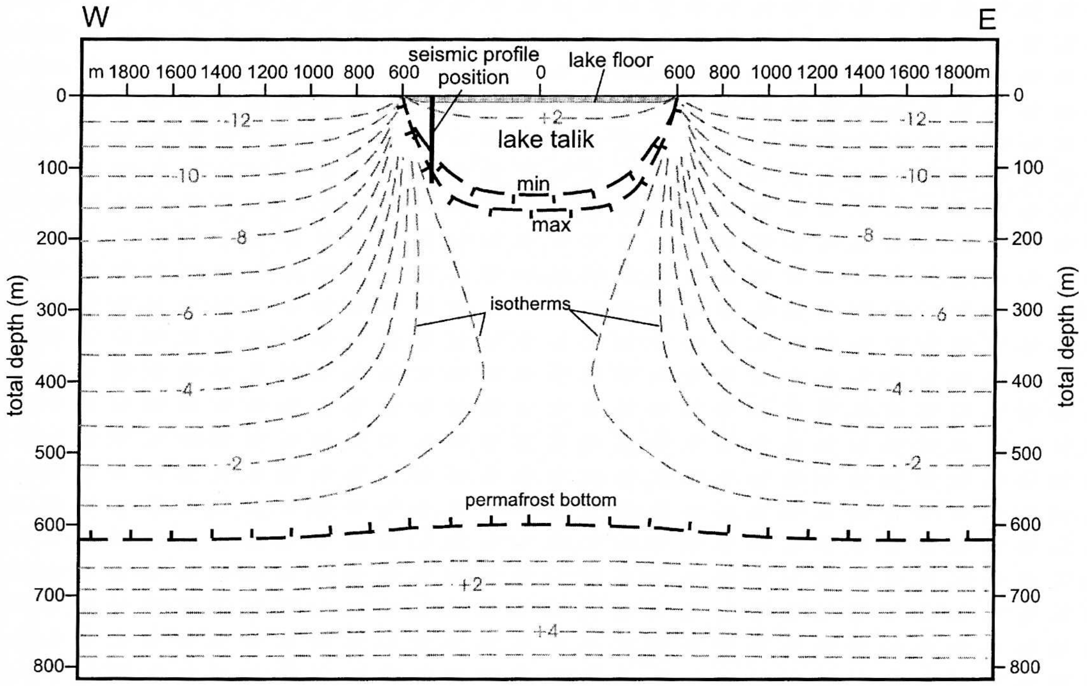

Fig. 8: Results of mathematical modeling of talik formation below one of Lake Nikolay´s sub-basins. The total depth (m) of the lake talik is dependent on the accepted thermophysical properties. Min. and max. results reflect the range originated by the different values of groups N1 through 3 (Tab. 1). Location of seismic profile from Fig. 7 is indicated. It has been gained perpendicular to the west-east oriented mathematical model.

Abb. 8: Ergebnisse der mathematischen Modellierung der Talik-Entstehung unter einem Teilbecken des Nikolay-Sees. Die Gesamttiefe des Talik ist abhängig von den akzeptierten thermophysikalischen Eigenschaften. Min.- und Max.-Ergebnisse geben den Bereich wieder, der aus den verschiedenen Werten der Gruppen N1 bis N3 entsteht (Tab. 1). Das seismische Profil aus Abb. 7 verläuft im rechten Winkel zum west-ost orientierten Schnitt des mathematischen Modells.

1.2 m) sediment structures are resolved down to a penetration depth of ca. 23 m with the 100 MHz antenna pair. The frozen sand as recovered in core A5 exhibits horizontal to slightly inclined reflectors in the radargram, probably representing fluvial bedding structures. The inclined bedding points towards the basin located at the southeastern end of the profile. This suggests that the thermokarst depression was established in the center of a former fluvial pathway.

CONCLUSIONS

We can reconstruct the following post-Pleistocene evolution of depositional processes in the Lake Nikolay area from our data set.

At 15,000-11,000 yr BP a continental sedimentation dominates the environment of Arga Island. Sandy deposits formed with high sedimentation rates indicate a fluvial environment under upper flow regime. Sediments underlying todays lake basins in the area consist of fine sand that is comparable with the surrounding sandy environment.

Gravitational sliding of marginal sediments into individual basins took place before lake sedimentation starts at about 7000 ^{14}C yr BP after a transition period from a fluvial to a shallow water to a limnic environment. The beginning of lake sedimentation coincides with the onset of the regional Holocene climatic optimum. Limnic sedimentation consisting of organic-rich sands in the center of the sub-basins takes place with average sedimentation rates of about 0.1 m per 1000 years.

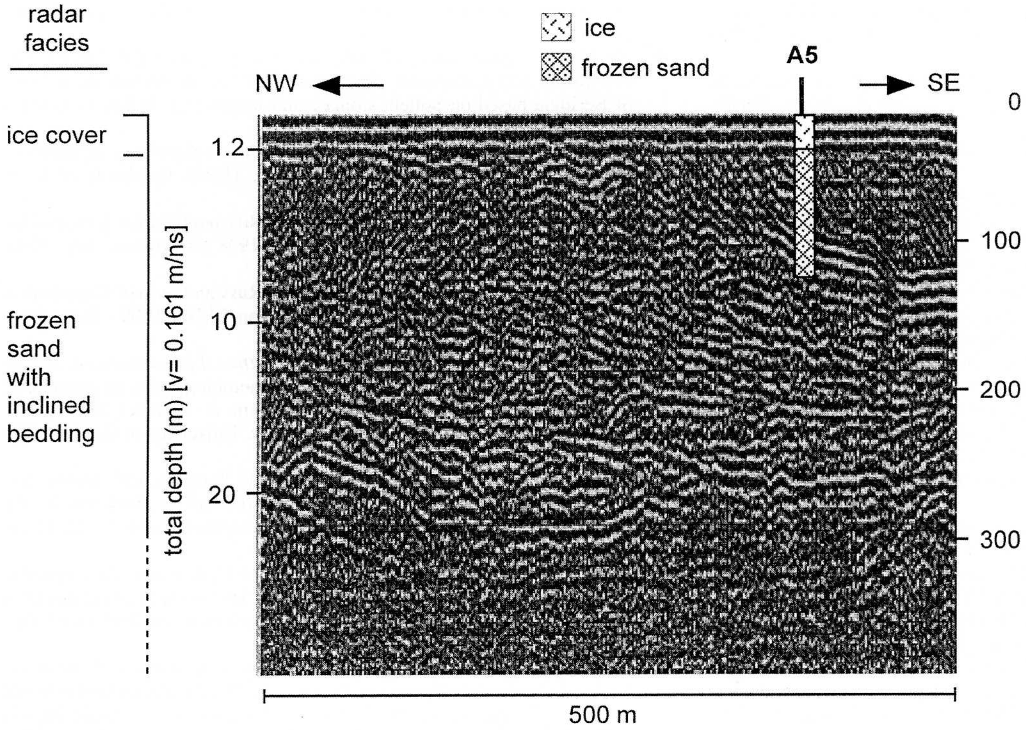

Fig. 9: Radar profile obtained with the 100 MHz antenna pair and drilling results of core A5.

Abb. 9: Radarprofil gemessen mit dem 100-MHz-Antennenpaar und Bohrergebnisse des Sedimentkerns A5.

Lake Nikolay has induced a talik expansion below its deeper basins. Mathematical modeling of the talik expansion supports the interpretation that subsidence of the thawed sandy subground alone is sufficient to have created the deeper basins on Arga Island even though the ice content is low in the subground. Neither geological (for example the occurrence of till, moraine) nor geophysical (for example the detection of glacial furrows or scratch marks) results are obtained, which support the hypothesis of a glacially caused morphology of the area as deduced from remote sensing techniques according to GROSSWALD et al. (1999). The occurrence of massive underground ice proposed by ARE & REIMNITZ (2000) cannot be proven by RES and shallow seismic measurements, either.

Presumably small ponds in abandoned fluvial pathways rather extended in depth and size due to thermokarst processes promoted in the ice-poor sandy subsurface. Thermokarst is still active especially at the northern shores where insolation is higher than at the southern shores and shore banks are retreating more rapidely due to thermoabrasion. This process promotes the elongation of the lake's shape. The spreading of the shorelines has merged several small thermokarst lakes together forming todays Lake Nikolay as the largest lake hold by the second terrace of the Lena River delta.

ACKNOWLEDGMENTS

The authors thank the captain, crew members and German-Russian field parties during expeditions Lena 98 and Lena 99. Special thanks are dedicated to the reviewers Erk Reimnitz and Martin Melles for essential improvements of the manuscript through their critical comments. Special thanks are also dedicated to Waldemar Schneider for crucial assistance during geophysical surveys. Ute Bastian, Maren Stapke and Lutz Schönicke are thanked for help in the lab, Christine Siegert for a graphical courtesy. This study is part of the German-Russian project "The Laptev Sea System", which was funded by the German Ministry of Education and Research (BMBF) and the Russian Ministry of Research and Technology.

References

Andreev, A.A. & Klimanov, V.A. (2000): Quantitative Holocene climatic reconstruction from Arctic Russia.- J. Paleolimnol. 24 (1): 81-91.

Andreev, A.A., Klimanov, V.A. & Sulerzhitsky, L.D. (2001): Vegetation and climate history of the Yana River lowland, Russia, during the last 6400 years.- Quaternary Sci. Rev. 20 (1-3): 259-266.

Andreev, A.A., Schirrmeister, L., Siegert, C., Bobrov, A.A., Demske, D. Seiffert, M. & Hubberten, H.-W. (2002): Paleoenvironmental changes in Northeastern Siberia during the Upper Quaternary - Evidence from pollen records of the Bykovsky Peninsula.- Polarforschung 70: 13-25.

Annan, A.P. & Davies, J.L. (1976): Impulse radar sounding in permafrost.- Radio Science 11: 383-394.

Are, F.E. & Reimnitz, E. (2000): An overview of the Lena River Delta setting: geology, tectonics, geomorphology, and hydrology.- J. Coastal Res. 16 (4): 1083-1093.

Ariztegui, D. & McKenzie, J.A. (1995): Temperature-dependent carbon-isotope fractionation of organic matter: a potential paleoclimatic indicator in Holocene lacustrine sequences.- In: B. FRENZEL (ed.), Problems of stable isotopes in tree-rings, lake sediments and peat-bogs as climatic evidence for the Holocene, Stuttgart, Gustav Fischer Verlag: 17-28.

Bauch, H., Kassens, H., Erlenkeuser, H., Grootes, P.M., Dehn, J., Peregovich, B. & Thiede, J. (1999): Depositional environment of the Laptev Sea (Arctic Siberia) during the Holocene.- Boreas 28: 194-204.

Berglund, B.E. & Ralska-Jasiveczowa, M. (1986): Pollen analysis and pollen diagrams.- In: B.E. BERGLUND (eds.), Handbook of Holocene paleoecology and paleohydrology, New York, Interscience: 455-484.

Boucsein, B., Fahl, K. & Stein, R. (2000): Variability of river discharge and Atlantic water inflow at the Laptev Sea continental margin during the past 15,000 years: implications from maceral and biomarker records.- Internat. J. Earth Sci. 89: 578-591.

Davies, J.L. & Annan, A.P. (1989): Ground-Penetrating-Radar for High-Resolution Mapping of Soil and Rock Stratigraphy.- Geophys. Prospecting 37: 531-551.

Ershov, E.D. (ed.) (1984): Thermalphysic properties of the rocks.- Moscow, MSU: 204 pp. (in Russian).

Eyles, N. & Mullins, H.T. (1997): Seismic-stratigraphy of Shuswap Lake, British Columbia, Canada.- Sed. Geol. 109: 283-303.

French, H.M. (1996): The periglacial environment. Longman, London. 121-124.

Føgri, K. & Iversen, J. (1989): Textbook of pollen analysis (4th Edition revised by K. FØGRI, P.E. KALAND & K. KRZYINSKI). Chichester, Wiley: 200 pp.

Fry, B., Brand, W., Mersch, F.J., Tholke, K. & Garritt, R. (1992): Automated analysis system for coupled $\delta^{13}C$ and $\delta^{15}N$ measurements.- Analyt. Chem. 64: 288-291.

Galabala, R.O. (1997): Perelekti and the initiation of glaciation in Siberia.- Quaternary Internat. 41/42: 152-171.

Gavrilov, A.V., Garagulya, L.S., Ershov, E.D. & Kondratyeva, K.A. (1986): Map of Regions showing conditions for frozen and unfrozen ground, 1:25,000,000, ISBN 0-9685013-0-3.

Gavrilov, A.V., Tumskoy, V.E. & Romanovskii, N.N. (2000): Mean annual ground temperature oscillation in the Laptev Sea region during the last 400 Kyr: method of paleotemperature curves compilation for mathematical simulation of terrestrial and offshore permafrost.- Rhythms of natural processes in the Earth cryosphere, Abstracts: 265-266 (in Russian).

Grigoriev, M.N. (1993): Criomorphogenesis in the Lena Delta.- Permafrost Institute Press, Yakutsk, Russia: 176 pp. (in Russian).

Grigoriev, M.N., Rachold, V. & Schwamborn, G. (2000): Problem of genesis and formation of the lakes (Arga-Muora-Sise Island, Northwest sector of the Lena Delta).- In: Proceedings International Conference Lakes of Cold Regions: 66-81 (in Russian).

Grosswald, M.G. (1998): Late-Weichselian ice sheets in Arctic and Pacific Siberia.- Quaternary Internat. 45/46: 3-18.

Grosswald, M.G. & Hughes, T.J. (1999): The Case For an Ice Shelf in the Pleistocene Arctic Ocean.- Polar Geography 23(1): 23-54.

Grosswald, M.G., Hughes, T.J. & Lasca, N.P. (1999): Oriented lake-and-ridge assemblages of the Arctic coastal plains: glacial landforms modified by thermokarst and solifluction.- Polar Record 35: 215-230.

Gundelwein, A. (1998): Eigenschaften und Umsetzung organischer Substanz in nordsibirischen Permafrostböden.- Hamburger Bodenkundliche Arbeiten 39: 162 pp.

Holmes, M.L. & Creager, J.S. (1974): Holocene history of the Laptev continental shelf.- In: Y. HERMAN (ed.), Marine Geology and Oceanography, Berlin, Springer Verlag: 211-229.

Judge, A.S., Tucker, C.M., Pilon, J.A. & Moorman, B.J. (1991): Remote Sensing of permafrost by ground-penetrating radar at two airports in Arctic Canada.- Arctic 44: 40-48.

Katasonov, E.M., Ivanov, M.S., Siegert, C., Katasonova, E.G. & Pudov, G.G. (1979): Structure and absolute geochronology of Alas deposits in Central Yakutia.- Novosibirsk, Nauka: 96 pp. (in Russian).

Katasonova, Y.G. & Ziegert, H.G. (1982): Slope sediments in river valleys of Central Yakutia.- In: Geology of the Cenozoic of Yakutia, Yakutsk, SO AN SSSR: 110-121 (in Russian).

Kearey, P. & Brooks, M. (1984): An introduction to geophysical exploration. Blackwell Scientific Publications: 296 pp.

Kleiber, H.P. & Niessen, F. (2000): Variations of continental discharge pattern in space and time: Implications from the Laptev Sea continental margin, Arctic Siberia.- Internat. J. Earth Sci. 89: 605-616.

Krbetschek, M.R., Gonser, G. & Schwamborn, G. (2001): Luminescence dating results of sediment sequences of the Lena Delta.- Polarforschung 70:

MacDonald, G.M., Velichko, A.A., Kremenetski, C.V., Borisova, O., Goleva, A.A., Andreev, A.A., Çwynar, L.C., Riding, R.T., Forman, S.L., Edwards, T.W.D., Aravena, R., Hammarlund, D., Szeicz, J.M. & Gattaulin, V.N. (2000): Holocene treeline history and climate change across northern Eurasia.- Quaternary Research 53: 302-311.

Meyer, H., Dereviagin, A., Siegert, C. & Hubberten, H.-W. (2002): Paleoclimate studies on Bykovsky Peninsula, North Siberia - Hydrogen and oxygen Isotopes in Ground Ice.- Polarforschung 70: 37-52.

Moorman, B.J. & Michel, F.A. (1997): Bathymetric mapping and sub-bottom profiling through lake ice with ground-penetrating radar.- J. Paleolimnol. 18: 61-73.

Müller, C. & Stein, R. (2000): Variability of fluvial sediments supply to the Laptev Sea continental margin during Late Weichselian to Holocene times: implications from clay mineral records.- Internat. J. Earth Sci. 89: 592-604.

Niessen, F. & Jarrard, R.D. (1998): Velocity and porosity of sediments from CRP-1 Drillhole, Ross Sea, Antarctica.- Terra Antarctica 5: 311-318.

Niessen, F. & Melles, M. (1995): Lacustrine sediment echosounding and physical properties.- In: H.-W. HUBBERTEN (ed.), The Expedition ARK-X/2 of RV Polarstern in 1994, Rep. Polar Res. 174: 69.

Panin, A.V., Sidorchuk, A.Y. & Chernov, A.V. (1999): Historical background to floodplain morphology: examples from the East European Plain.- In: S.B. MARRIOTT & J. ALEXANDER (eds.), Floodplains: Interdisciplinary Approaches, Geol. Soc London Spec. Publ. 163: 217-229.

Petit, J.R., Jouzel, J., Raynaud, D., Barkov, N.I., Barnola, J.-M., Basile, I., Bender, M., Chappellaz, J., Davis, M., Delaygue, G., Delmotte, M., Kotlyakov, V.M., Legrand, M., Lipenkov, V.Y., Lorius, C., Pépin, L., Ritz, C., Saltzman, E. & Stievenard, M. (1999): Climate and atmospheric history of the past 420,000 years from the Vostok ice core, Antarctica.- Nature 399: 429-436.

Pisaric, M.F.J., MacDonald, G.M., Velichko, A.A. & Cwynar, L.C. (2001): The late-glacial and post-glacial vegetation history of the northwestern limits of Beringia based on pollen, stomate and megafossil evidence.- Quaternary Sci. Rev. 20: 235-245.

Quinn, R.J. (1997): Marine high-resolution reflection seismology: acquisition, processing and applications. Unpubl. Ph.D. Thesis, University of Southampton.

Rachold, V. & Grigoriev, M.N. (eds.) (1999): Russian-German Cooperation System Laptev Sea 2000: The Lena Delta 1998 Expedition.- Rep. Polar Res. 315: 259 pp.

Rachold, V. & Grigoriev, M.N. (eds.) (2000): Russian-German Cooperation SYSTEM Laptev Sea 2000: The Expedition LENA 1999.- Rep. Polar Res. 354: 269 pp.

Robinson, S.D., Burgess, M.M., Judge, A.S., Kettles, I.M., Moorman, B.J. & Wolfe, S.A. (1997): The use of ground penetrating radar in permafrost environments: recent applications.- Program & Abstract 27th Arctic Workshop, 1997, Department of Geography, University of Ottawa: 191-193.

Romanovskii, N.N., Kholodov, A.L., Gavrilov, A.V., Tumskoy, V.E., Hubberten, H.W. & Kassens, H. (1999): Ice-bonded permafrost thickness in the eastern part of the Laptev Sea shelf.- Kryosphera Zemli 3: 22-32 (in Russian).

Romanovskii, N.N., Hubberten, H.W., Gavrilov, A.V., Tumskoy, V.E., Tipenko, G.S., Grigoriev, M.N. & Siegert, C. (2000): Thermokarst and land-ocean interactions, Laptev Sea region, Russia.- Permafrost and Periglacial Processes 11: 137-152.

Schirrmeister, L., Siegert, C., Meyer, H., Derevyagin, A., Kienast, F., Andreev, A., Kunitsky, V., Tumskoy, V. & Grootes, P. (2000): Paleoenvironmental and paleoclimatic records from permafrost deposits in the Arctic Region of Northern Siberia.- In: Proceedings Intern. Conference on Past Global Changes, Prague, GeoLines 11, Institute of Geology, AS CR: 147-150.

Schwamborn, G., Schneider, W., Grigoriev, M.N., Rachold, V. & Antonow, M. (1999): Sedimentation and environmental history of the Lena Delta.- In: V. RACHOLD & M.N. GRIGORIEV (eds.), Expeditions in Siberia in 1998, Rep. Polar Res. 315: 94-111.

Schwamborn, G., Rachold, V., Grigoriev, M.N. & Krbetschek, M. (2000a): Late Quaternary sedimentation history of the Lena Delta.- In: Proceedings Intern. Conference on Past Global Changes, Prague, GeoLines 11, Institute of Geology, AS CR: 35-38.

Schwamborn, G., Schneider, W., Grigoriev, M.N., Rachold, V. & Antonow, M. (2000b): Sedimentation and environmental history of the Lena Delta.- In: V. RACHOLD & M.N. GRIGORIEV (eds.), The Expedition LENA 1999, Rep. Polar Res. 354: 57-64.

Schwamborn, G., Rachold, V., Schneider, W., Grigoriev, M. & Nixdorf, U. (2000c): Ground penetrating radar and shallow seismic-Stratigraphic and Permafrost Investigations of Lake Nikolay, Lena Delta, Arctic Siberia.- Proceedings 8th Internat. Conf. Ground Penetrating Radar, SPIE Vol. 4084: 783-789.

Sheriff, R.E. & Geldart, L.P. (1995): Exploration seismology. Cambridge University Press: 592 pp.

Sidorchuk, A.Y., Panin, A.V., Borisova, O.K., Elias, S.A. & Syvistki, J.P. (2000): Channel morphology and river flow in the northern Russian Plain in the Late Glacial and Holocene.- Internat. J. Earth Sci. 89: 541-549.

Siegert, C. (1999): Late Quaternary denudation processes in permafrost landscapes of Central Siberia and their impact on the Arctic Ocean.- In: Abstracts, 3rd QUEEN Workshop Oeystese, Norway.

Siegert, C., Derevyagin, A.Y., Shilova, G.N., Hermichen, W.-D. & Hiller, A. (1999): Paleoclimatic indicators from permafrost sequences in the eastern Taymyr lowland.- In: H. KASSENS, H.A. BAUCH, I.A. DMITRENKO, H. EICKEN, H.-W. HUBBERTEN, M. MELLES, J. THIEDE & L.A. TIMOKHOV (eds.), Land-ocean systems in the Siberian Arctic: dynamics and history, Berlin, Springer-Verlag: 477-502.

Siegert, C., Schirrmeister, L. & Babiy, O. (2002): The sedimentological, mineralogical and geochemical composition of Late Pleistocene deposits from the Ice Complex of the Bykovsky Peninsula, Northern Siberia.- Polarforschung 70: 3-11.

Spielhagen, R., Erlenkeuser, H. & Heinemeier, J. (1998): Deglacial freshwater outflow from Lena River (Siberia). - In: Abstracts, 2nd QUEEN Workshop, St. Petersburg, 48.

Stuiver, M., Reimer, P.J., Bard, E., Beck, J.W., Burr, G.S., Hughen, K.A., Cromer, B., McCormic, G., van der Plicht, J. & Spurk, M. (1998): INTCAL 98 radiocarbon age calibration, 24,000-0 cal BP.- Radiocarbon 40: 1041-1083.

Zimmerman, R.W. & King, M.S. (1986): The effect of the extent of freezing on seismic velocities in unconsolidated permafrost.- Geophysics 51: 1285-1290.